BAIUST Academic Journal (BAJ), Volume 4, Issue 1, 2023: 1–13
https://doi.org/10.63307/BAJ.4.1.S1

Numerical Analysis of Soil–Pile Interface Properties of Bored Pile Embedded in Silty Clay Soils

Md. Mohshin Ali*, Md. Mahi Abrar, Md. Abiduzzaman, and Sonjoy Deb Nath

Department of Civil Engineering, Bangladesh Army University of Engineering and Technology (BAUET), Natore, Bangladesh. E-mail: mmali19bd @gmail.com

*Corresponding Author

Abstract: Pile foundations are regarded as a highly sophisticated domain within the discipline of geotechnical engineering and are progressively gaining recognition as a cost-effective foundation technique for skyscrapers. Traditional empirical methods, CPT-based analysis and pile load tests are used to predict the load-displacement response and load transfer mechanisms along the length of the pile. However, these methods may not be suitable for piles and soil conditions different from those for which the methods were developed. Under such conditions, numerical analysis using soil properties measured from in situ soil tests can be an effective approach to obtain shear stress along the pile axis (t) and pile displacement (z) along the pile (t-z curves) for predicting pile movements under axial load. This paper describes the numerical analysis, presents the soil–pile interface properties including allowable capacity, axial force, vertical stress, and settlement behavior of bored piles embedded in silty clay soils and highlights the benefits of the proposed simple and time-efficient numerical approach. The numerical modeling was developed in AllPile 6.5.0V software to evaluate the performance of bored piles embedded in silty clay soils that were characterized by SPT. The results of the analysis showed that numerical analysis can better predict the response of soil-piles compared to empirical and/or theoretical analysis to optimize pile design and construction.

Keywords: Bored Pile, AllPile, soil-pile interface, t-z curve, SPT

1. Introduction

Pile foundation is considered as one of the state-of-the-art areas of geotechnical engineering (Chanda et al., 2023). In most civil engineering projects, superstructure loads are transferred to the ground through foundations, which can be either spread or piled. The need for a deep foundation in any project usually results from several factors, including subsurface conditions, foundation loads, and acceptable foundation settlement criteria (Bell et al., 2002). Once the decision has been made to mainly use a deep foundation, the next step is to choose the type of pile and design the pile. In addition to local experience and practice, the choice of pile type is often based on soil conditions, while the initial choice of pile size and length is usually based on static pile load capacity calculations. High-rise buildings are usually founded on some form of piled foundation which is subjected to a combination of vertical, lateral, and overturning forces (Poulos, 2011) to transfer the structural reactions through the weak and low-bearing soil strata to the deeper and harder layers of the soil.

There are many different types of piles invented with the main purpose of satisfying the structural, soil, and local environmental and economic conditions. All of them can be applied using two main installation techniques: as driven or bored piles (Day, 2010). The method of activating pile bearing capacity varies and is affected by many factors such as pile types, soil characteristics, drilling or driving method, loading method, etc. The bearing capacity of piles usually consists of two parts: pile shaft resistance and pile tip resistance. The resistance of the pile axis is most sensitive to the pile-bearing capacity calculation process, which results from the friction of the pile surface and/or the cohesion-adhesion between the pile and the soil (Yu, 2009; Hannigan et al., 1998). The calculation method is developed for the two most typical soil types: cohesionless (sand) and cohesive (clay).

However, very often the soil is not easily distinguished and spreads not only in several layers but also as mutually mixed combinations of cohesive and cohesionless soils. Capillarity can cause foundation soils to become heavily saturated, reducing pile-bearing capacity. In such instances, the difficulty of selecting the standard techniques of calculating approach becomes extremely complex when all of the governing aspects are considered. Besides conventional methods are time-consuming and costly as well as provide no soil-pile interface properties. Pile load tests and cone penetration tests are also expensive and time-consuming, and many empirical or semi-empirical methods have been developed to avoid them (Sliwinski & Fleming, 1984). However, the most uncertain about this issue is the basic approach to pile resistance calculation, which is defined as the allowable stresses and ultimate limit design approach. Methods based on allowable stresses are traditional, well-established, and mostly applied, but conservative, using high global safety factors of 2-4 (Becker, 1997). The ultimate limit design method is more rational, but still considered risky, not acceptable for many designers, and therefore, not included in many codes and standards (Becker, 1997). Nowadays, the situation clearly shows the global existence of unresolved uncertainties in the pile load-bearing capacity calculation (Christian & Baecher, 2011). As a result, the only approach for researchers and design engineers to obtain a reliable estimate of pile-bearing capacity is to conduct a cost-effective and time-efficient numerical analysis of piles in c- f soils along with surface influence factors.

The interactions between piles and the surrounding soil are complex, and broad generalizations about pile behavior are unrealistic. Insertion of piles alters the character of the soil and intense strains are set up locally near the piles (Rao & Supriya, 2015). The non-homogeneity of soils, besides the impacts of pile diameter and depth, includes further

https://doi.org/10.63307/BAJ.4.1.S1

difficulties in the understanding of soil-pile interaction (Rao & Supriya, 2015). In such cases, an understanding of the pile capacity and other soil-pile interface properties of bored piles in soft clay soils is required to be successful in the design of pile foundations. Therefore, it is of great interest for researchers and designers to know the pile capacity, shear stress, displacement along the soil-pile interface, and load-settlement behavior of bored piles in silty clay soils under vertical loading.

Several previous works have studied the influence of foundation geometry (Garcia & Albuquerque, 2019; Bezerra et al., 2005), the contribution of raft-soil contact and load distribution among the elements and their variables (Butterfield & Banerjee, 1971), and the use of numerical models for analysis of pile (Ottaviani, 1975). The parameters involving foundation geometry, number of piles, and material properties influence the behavior of the foundation (Poulos & Davis, 1980). Most researchers mainly focus on the influence of foundation geometry, number of piles, and material properties on the performance of pile foundations. In this context, numerical modeling of pile foundations including soil and pile properties and soil-pile interface properties after analysis will be presented. In this study, a numerical model was developed using AllPile 6.5.0V software to predict the ultimate capacity of a pile when embedded in silty clay soil. This work provides insight into the performance of bored piles driven into clay soil so that pile foundations can be properly designed. This paper also focuses on the use of AllPile 6.5.0V software to measure t-z curves at the soil-pile interface and the effectiveness of this approach in predicting load displacement and load transfer mechanisms using numerical analysis results investigated with RCC bored piles driven into silty clay soils.

2. Materials and Methods

2.1 Pile Profile and Properties Used

In this study, a bored pile of 50 ft. in length and 16 in. diameter embedded in silty clay soils was modeled in the AllPile V6.5.0 commercial program. The pile properties and profile used in this investigation are presented in Table 1 and Figure 1.

Table 1
RCC Bored Pile Properties Used in this Investigation

Depth (ft.)	Width (in.)	Area (in.^{2})	Perimeter (in.)	I (in.^{4})	E (kip/ in.^{2})	Weight (kip/ft.)
0.0	16	201.1	50.3	3217.0	3000	0.209
50.0	16	201.1	50.3	3217.0	3000	0.209

Figure 1
Loads and Profile of RCC Bored Pile Properties

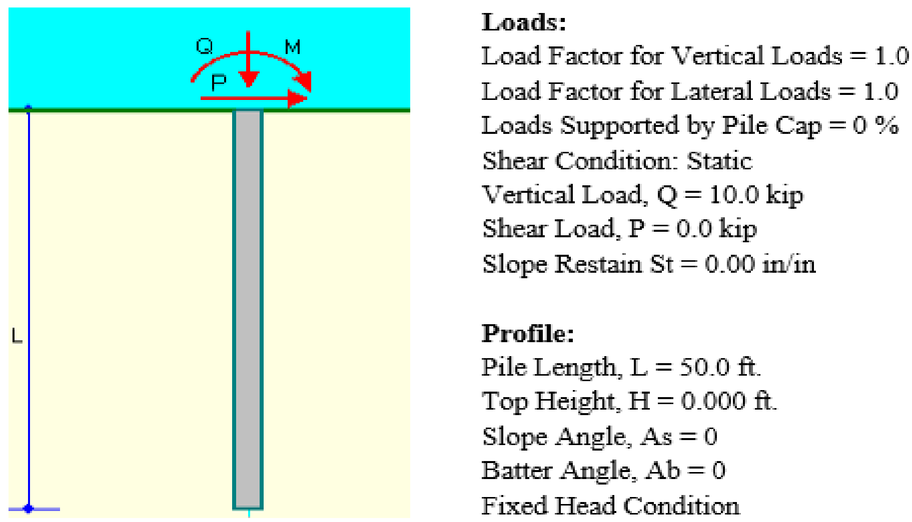

2.2 Properties of Soil Used

Studying the strength of soft silty clay soils is very important in geotechnical design. Soil particles such as clay, sand, and silt play an important role in determining soil behavior. The behavior of clay and sand particles is unique; however, the behavior of silt particles is in a transitional form between sand and clay. Therefore, in this paper, the silty clay soil was modeled with the bore log (including soil stratification) and parameters as shown in Table 2 and Figure 2.

Table 2
Properties of Soils Used in this Investigation

Zg (m)	Soil Data Input	G (lb/ft.^{3})	Phi	Cu, Undrained (kip/ft.^{2})	K (lb/in.^{3})	E50 or Dr	Nspt
0	Soft Clay	96.4	0.00	0.09	9.7	4.38	1
6.5	Sand/Gravel [W]	38.1	27.2	0.00	4.3	8.69	2
10	Silt (Phi+C) [W]	56.8	27.6	0.31	95.5	1.33	5
20	Silt (Phi+C) [W]	68.6	30.7	0.78	431.1	0.76	13
26	Silt (Phi+C) [W]	64.7	29.1	0.52	236.2	0.98	8
30	Silt (Phi+C) [W]	66.2	29.6	0.59	285.6	0.91	9
36	Silt (Phi+C) [W]	64.2	29.0	0.50	222.9	1.00	8
40	Stiff Clay [W]	68.8	0.00	1.63	455.4	0.74	13
45	Stiff Clay [W]	130.3	0.00	1.40	369.0	0.81	11
50	Stiff Clay [W]	129.3	0.00	1.26	317.7	0.87	10

https://doi.org/10.63307/BAJ.4.1.S1

The effective friction angle increases up to 33.5^0 depending on the silt content or density (Zhongkun & Paul, 2017). The relationship between the silt content and effective angles of friction is proportional as stated by Liu et al. (2021).

Figure 2

Bore log Graph with Soil Stratification Used in this Investigation

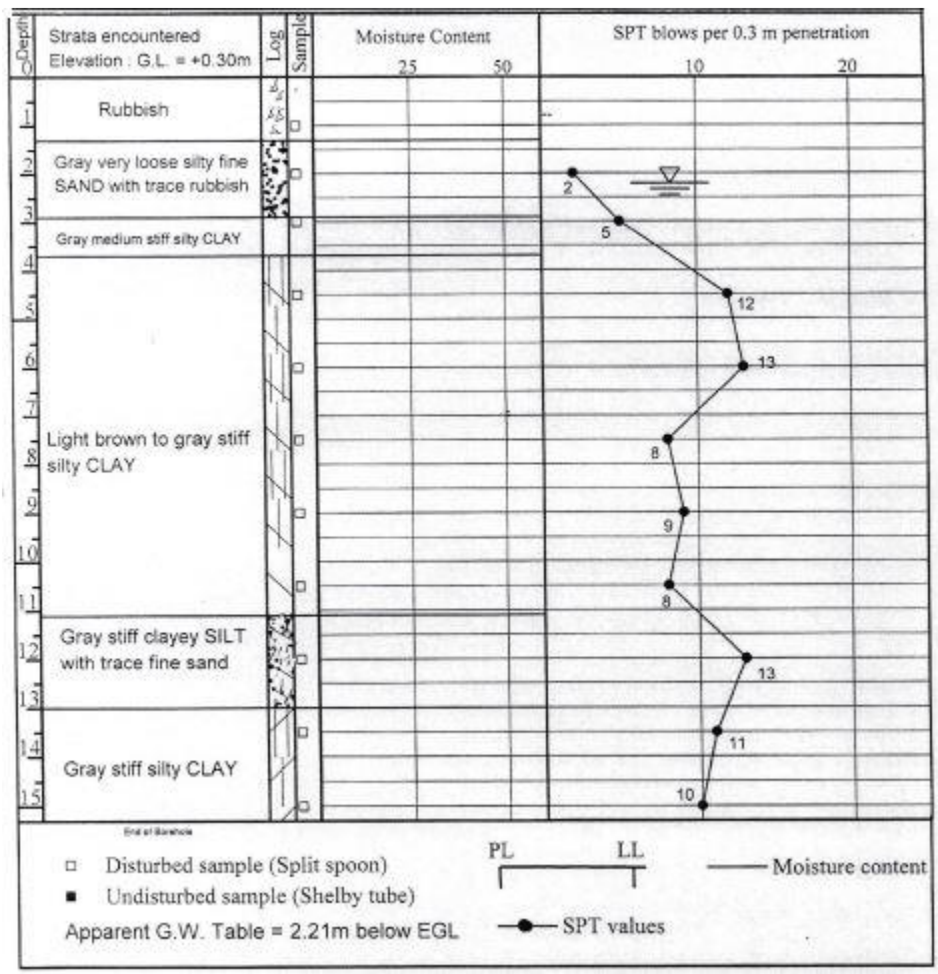

2.3 Features of AllPile Software and Numerical Modeling

AllPile 6.5.0V is a Windows-based analysis program that handles virtually all types of piles, including steel pipes, H-piles, pre-cast concrete piles, auger-cast piles, drilled shafts, timber piles, jetted piles, tapered piles, piers with bell, micro piles, uplift anchors, uplift plate, and shallow foundations. One of the major advantages AllPile 6.5.0V has over other pile software is that it combines most pile analyses in a single program. It calculates compression (with settlement), uplift, lateral capacity, and group analysis all together. Users only have to enter information once instead of several times in different programs. AllPile 6.5.0V makes pile analysis easy, economical, and time-efficient. AllPile 6.5.0V is suitable for all engineers, even those without too much pile analysis experience. It helps structural engineers choose soil parameters, and geotechnical engineers choose pile properties. AllPile 6.5.0V is a must-have tool for structural, geotechnical, and construction engineers for numerical analysis of all types of piles and shallow foundations.

2.4 Methodology

The steps followed for the research are shown in the following flowchart:

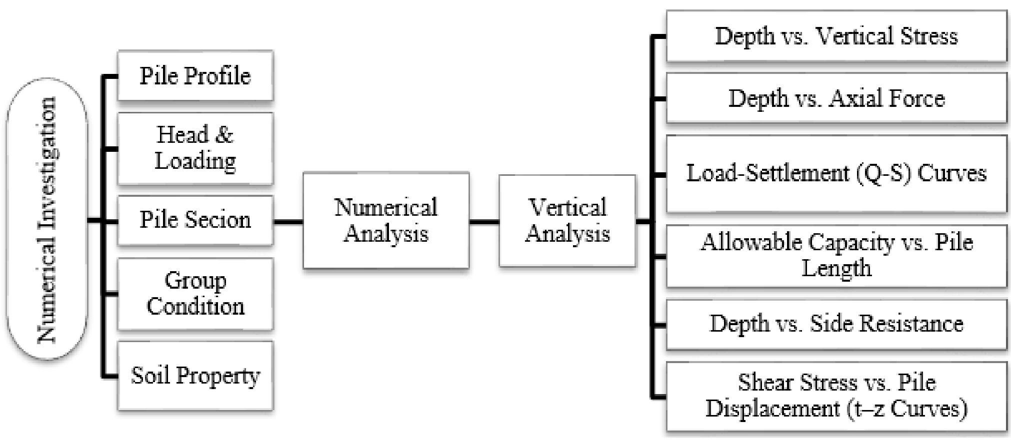

3. Validation of the Numerical Model

The validity of the numerical model employed in the study was verified by comparing it with two different published cases. The details of these two cases are presented in the following sub-sections.

Case Study 1 (Abdel Salam et al., 2012)

Abdel Salam et al., (2012) discussed the development and use of a modified borehole displacement test (MBST) to improve the prediction of the load displacement and load distribution response of axially loaded piles in clay soils using the load transfer analysis method (i.e., t. –z analysis). The test piles were axially loaded up to 440 kips with a hydraulic jack and the applied load was measured with a 290 kips load cell. The piles were subjected to a load test according to the rapid test procedure described in ASTM D1143 (ASTM 2007). Almost the same results were found while comparing the results of this study with the measurement results reported by Abdel Salam et al., 2012 and is shown in Figure 3.

https://doi.org/10.63307/BAJ.4.1.S1

Figure 3

Comparison of t-z Curves between the Present Study and the Measured Results Reported by Abdel Salam et al. (2012)

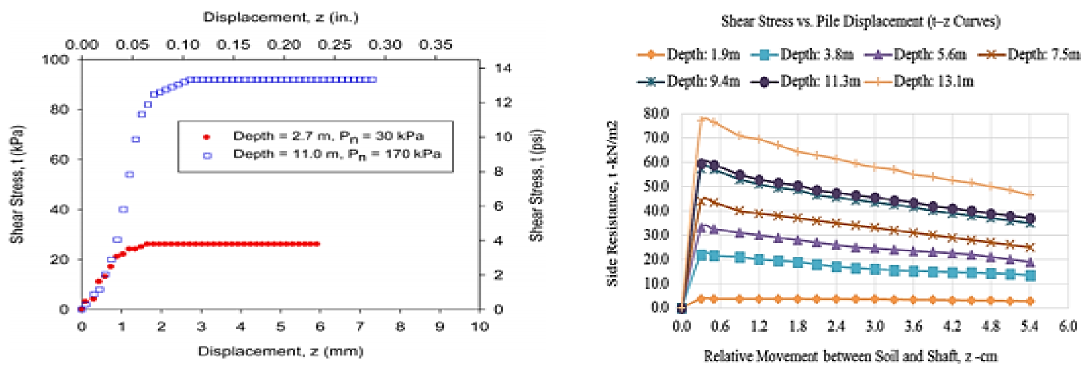

(a) t-z curves for the soil–pile interface measured using mBST (Abdel Salam et al., 2012).

(b) t-z curves for the soil–pile interface measured using numerical model (Present Study).

Case Study 2 (Chik et al., 2009)

Chik et al. (2009) studied large diameter 1.2 m boring piles used to construct a new 2.2 km long two-lane road viaduct over an existing road. The road project is located in Port Klang and connects the West Harbor with Kuala Lumpur, Malaysia. To evaluate the axial bearing capacity of the designed piles, the piles were tested vertically. Each boring pile is approximately 75 m long and the boring piles are designed to withstand loads between 300 and 600 kN. The subsurface is generally characterized by a soft silty clay about 20m deep, under which is a layer of soft silty clay 10m thick, followed by medium to dense silty sand and medium silty sand followed by a layer of hard silty clay. Almost the same results were found while comparing the results of this study with the measurement results reported by Chik et al. (2009) are shown in Figure 4.

Figure 4

Comparison of Load-Settlement Curves between the Present Study and the Measured Results Reported by Chik et al. (2009)

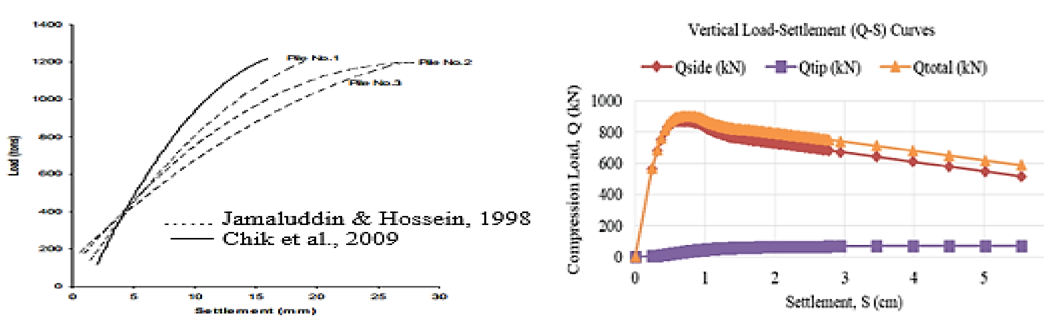

(a) Load-Settlement Curves (Chik et al., 2009)

(b) Load-Settlement Curves (Present Study)

4. Results and Discussions

4.1 Effective Vertical Stress in the Soil Adjacent to the Pile with Depth

Figure 5 represents the variation of vertical stress in the soil adjacent to the bored cast in-situ pile in silty clayey soils under vertical analysis.

Figure 5
Variation of Effective Vertical Stress in the Soil Adjacent to the Pile with Depth.

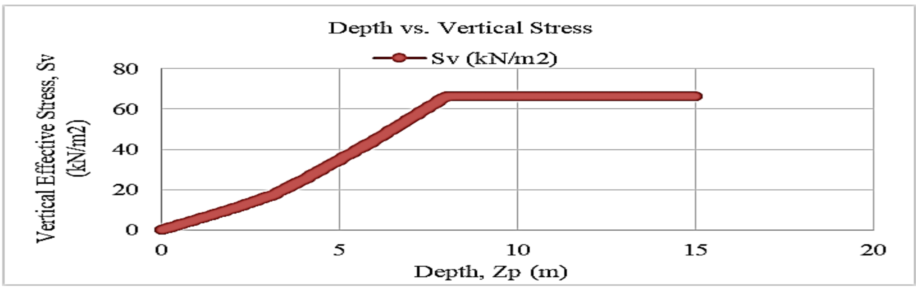

The effective vertical stress increases as depth increases until a certain depth of penetration is reached. Below this depth, which is called critical depth and denoted Dc, effective vertical stress more or less remains constant (Figure 5). The stress increases linearly up to 8m depth and then becomes constant. This is because the overburden stress has reached a maximum limit at critical depth (Dc).

4.2 Axial Force Distribution along the Embedded Depth of Piles

The distribution of axial force along the embedded depth of piles is shown in Figure 6. The maximum value of the axial force occurs at the pile head and then decreases gradually with depth. The uplift axial force/ ultimate uplift capacity (Qup) of the BCIS pile was found to be 780.30 kN, whereas, the downward axial force/ultimate downward (compression) capacity (Qdw) of the bored pile was found to be 903.10 kN.

Figure 6
Axial Force Distribution along the Embedded Depth of Piles

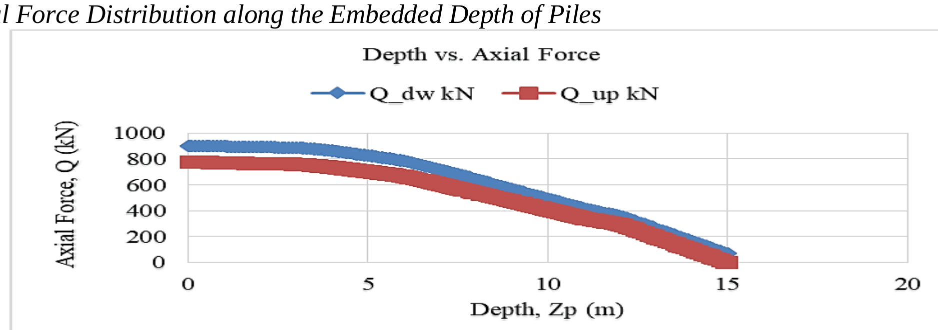

https://doi.org/10.63307/BAJ.4.1.S1

4.3 Vertical Load-Settlement (Q-S) Curves for Bored Pile in Silty Clayey Soils

Figure 7 represents the load-settlement curves (Q-S curves) of a cast in-situ pile in silty clayey soils under vertical loading. The initial steeper portion of the load settlement curve indicates that the pile would have a lesser settlement for a given load.

Figure 7

Load-Settlement (Q-S) Curves for BCIS Pile in Silty Clayey Soils

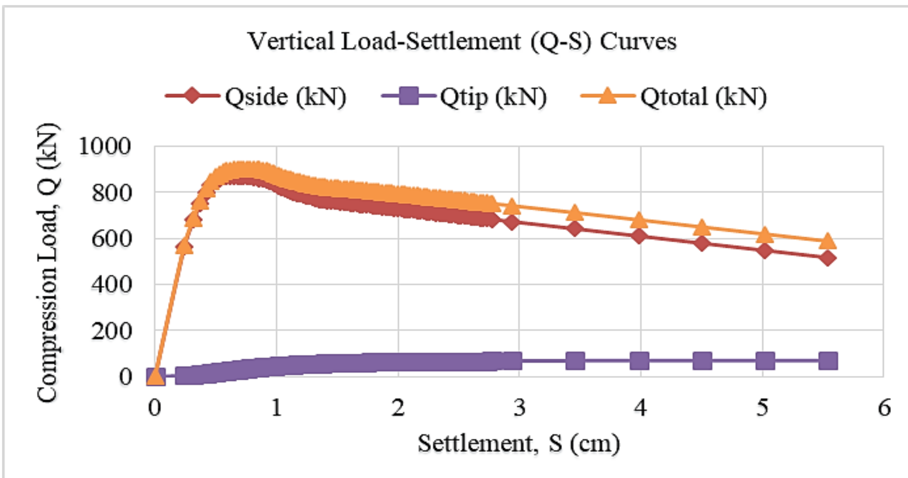

The overall vertical bearing capacity/total ultimate capacity of the bored pile was found to be 903.10 kN with a little settlement of 0.78 cm (i.e. 7.8 mm) and beyond this, a large settlement was observed without increasing of ultimate capacity. The reduction of ultimate capacity may be due to skin friction between soil and pile. A portion of the pile was absorbed by soil skin friction, resulting in a downward force that increases loading on shaft piles and reduces the bearing capacity of the piles and finally shear failure is pronounced in soil mass.

4.4 Variation of Allowable Capacity with Pile Length

The variation of allowable downward capacity (Qd) and uplift capacity (Qu) with pile length (L) is shown in Figure 8. The analysis results revealed that the allowable capacity (Qd and Qu) increased linearly with the increased depth of the pile. The allowable uplift capacity of the bored pile was found to be 315.5 kN, whereas, the allowable downward capacity was found to be 364.48 kN when the length of the pile was 15 m, embedded in silty clayey soils.

Figure 8
Variation of Allowable Capacity with Pile Length

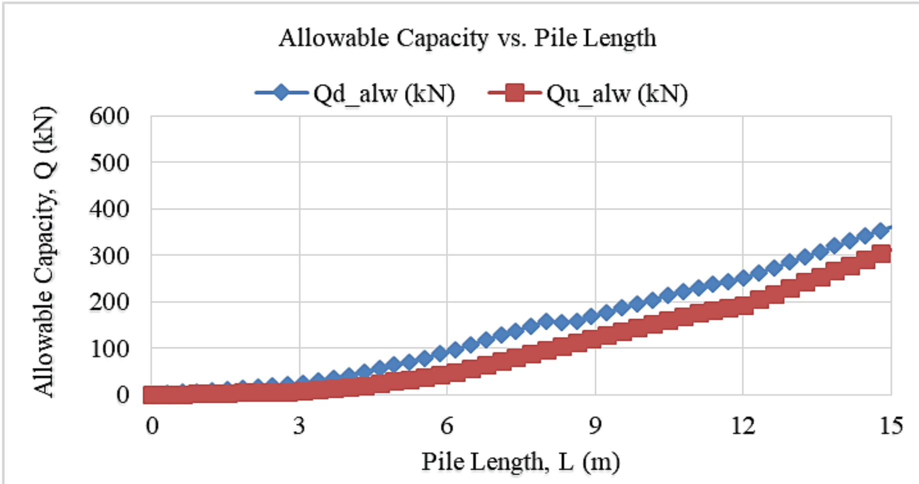

4.5 Variation of Skin Friction (Side Resistances and Adhesion) between Soil and Pile

The pile side friction curve is formulated and is presented in Figure 9. The pile side friction increases gradually with the increased depth of the pile.

Figure 9
Variation of Side Resistances (Uplift and Downward) between Soil and Pile

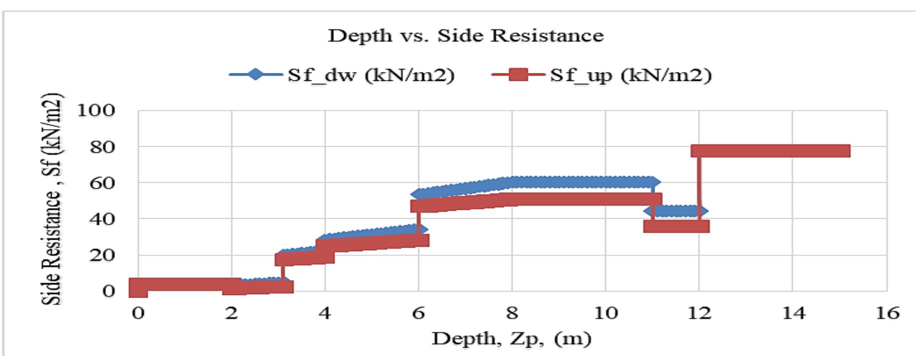

This is because during the load transfer process, as the depth increases, the pile side friction resistance gradually works and reaches the maximum level until the pile top load begins to be mainly borne by the pile tip resistance. Since the investigated soil profile is soft silty clay, the frictional resistance offered by the soil surrounding the pile is dominated over the tip resistance and consequently increases gradually. Moreover, the adhesion between pile and soil plays a prominent role in increasing the side resistance of piles in clays in terms of total stresses.

https://doi.org/10.63307/BAJ.4.1.S1

4.6 Relationship between Shear Stress at the Pile Shaft (t) and Pile Displacement (z) along the Pile Shaft

Figure 10 represents the relationship between shear stress and displacement (t–z curves) of the soil–pile interface at a specific depth (1.9m, 3.8m, 5.6m, 7.5m, 9.4m, 11.3m, and 13.1m) along the pile length. The largest side resistance (t) was found to be at a depth of 13.1 m, while the lowest side resistance (t) was found to be at a depth of 1.9 m. That means the soil shear strength at a depth of 13.1 m is larger than that of at 1.9 m. The analysis results also revealed that the maximum movement/pile displacement (Zm) at the pile head to fully mobilized shear strength was around 3.0 - 5.0 mm.

Figure 10

Relationships between Shear Stress at the Pile Shaft (t) and Pile Displacement (z) along the Pile Length

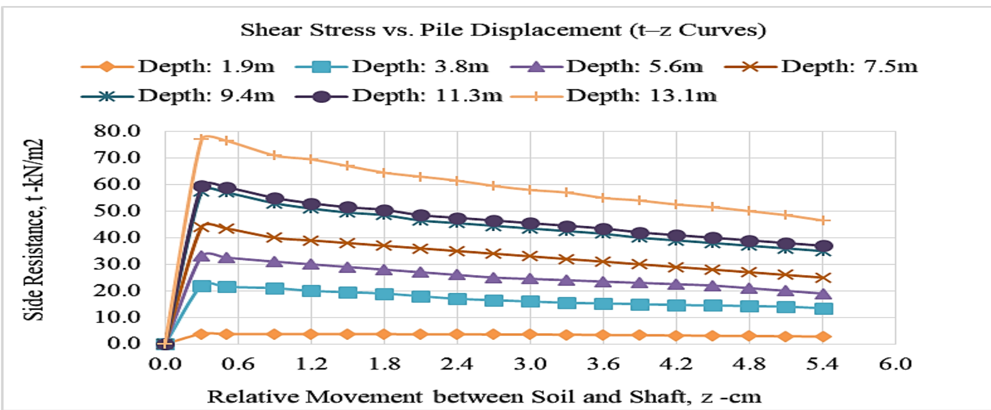

5. Conclusion and Recommendation

5.1 Conclusion

Based on the results presented in this research, the major findings can be summarized as follows:

1. Engineers will be able to accurately determine the critical depth through numerical analysis considering the controlling factors such as soil type, pile diameter, and installation techniques to ensure the stability and safety of structures supported by piles.
2. Based on numerical analysis, the maximum value of ultimate uplift capacity (Qup) and ultimate downward capacity (Qdw) of the bored pile was found to be 780.30 kN and 903.10 kN respectively.
3. Based on the load-settlement curve, the overall vertical bearing capacity/total ultimate capacity of the bored pile was also found to be 903.10 kN with a little settlement of 7.8 mm beyond which a large settlement was observed without increasing of ultimate capacity.

4. The allowable uplift and downward capacity of the bored pile were found to be 315.5 kN and 364.48 kN respectively when the length of the pile was 15 m.
5. The frictional resistance offered by the soil surrounding the pile embedded in soft silty clay was found to be dominant over the tip resistance and consequently increased gradually as the depth increased.
6. The maximum movement/pile displacement (Zm) to fully mobilized shear strength was found to be 3.0-5.0 mm.
7. Designers and researchers may use simplified "t-z" curves at a specific depth derived from numerical analysis as an alternative to analytical and/or empirical "t-z" curves from in-situ tests that are limited to predefined test configurations (Coyle & Reese 1966; Vijayvergiya, 1977).
8. The proposed numerical analysis is a simple and cost-effective solution that efficiently captures the soil–pile interface properties and helps to optimize the design and construction of piles.

5.2 Recommendation

Structural, geotechnical, and construction engineers may use simple and time-efficient AllPile 6.5.0V software for numerical analysis of soil–pile interface properties of all types of pile foundations in which only bore log data with soil stratification is used for once.

References

ASTM D1143-07. (2007). *Standard Test Methods for Deep Foundations under Static Axial Compressive Load*. ASTM International.

Becker, D. E. (1997). Eighteenth Canadian geotechnical colloquium: Limit states design for foundations. Part II. Development for the national building code of Canada. *Canadian Geotechnical Journal, 33*(6), 984–1007.

Becker, D. E. (1997). Eighteenth Canadian geotechnical colloquium: Limit states design for foundations. Part I. An overview of the foundation design process. *Canadian Geotechnical Journal*, 33(6), 956–983.

Bell, K. R., Davie, J. R., Clemente, J. L., & Likins, G. (2002). Proven success for driven pile foundations. In *Deep Foundations 2002: An International Perspective on Theory, Design, Construction, and Performance* (pp. 1029–1037).

Bezerra, J. E., Da Cunha, R. P., & Sales, M. M. (2005). Optimization concepts for the design of piled raft foundation systems. 16th Int. Conf. *Soil Mech. and Geotech. Eng*., pp. 1947–1950. http://dx.doi.org/10.3233/978-1-61499-656-9-1947

Canakci, H. (2007). Pile foundation design using Microsoft Excel. *Computer Applications in Engineering Education*, 15(4), 355–366.

Chanda, D., Saha, R., Haldar, S., & Choudhury, D. (2023). State-of-the-art review on responses of combined piled raft foundation subjected to seismic loads using static and dynamic approaches. *Soil Dynamics and Earthquake Engineering*, 169, 107869.

https://doi.org/10.63307/BAJ.4.1.S1

Chik, Z. H., Abbas, J. M., Taha, M. R., & Shafiqu, Q. S. (2009). Lateral behavior of single pile in cohesionless soil subjected to both vertical and horizontal loads. *European Journal of Scientific Research*, 29 (2), 194–205.

Christian, J. T., & Baecher, G. B. (2011). Unresolved problems in geotechnical risk and reliability. In *Geo-Risk 2011: Risk Assessment and Management* (pp. 50–63).

Coyle H. M., & Reese L. C. (1966). Load transfer for axially loaded piles in clay. *Journal of the Soil Mechanics and Foundations Division, ASCE*, 92(2), 1–26.

Day, R. W. (2010). *Foundation engineering handbook: design and construction with the 2009 international building code*. McGraw-Hill Education.

Garcia, J. R., & De Albuquerque, P. J. R. (2019). Analysis of the contribution of the block-soil contact in piled foundations. *Latin American Journal of Solids and Structures*, 16(6), 1–22.

Hannigan, P. J., Goble, G. G., Thendean, G., Likins, G. E., & Rausche, F. (1998). *Design and construction of driven pile foundations*, volume I (No. FHWA-Hl-97-013). United States. Federal Highway Administration. Office of Technology Applications.

Jamaludin, A., & Hussein, A. N. (1998). The performance of large diameter bored piles used for road project in Malaysia. *Proceedings of the 3rd International Geotechnical Seminar on Deep Foundation on Bored and Auger Piles, Ghent, Belgium*, 19-21 October, pp: 335–338.

Liu, Y.; Liu, Z.; Oh, E.; & Ong, D. E. L. (2021). Strength and microstructural assessment of reconstituted and stabilised soft soils with varying silt contents. *Geosciences*, 11 (302). https://doi.org/10.3390/ geosciences11080302

Ottaviani, M. (1975). Three-dimensional finite element analysis of vertically loaded pile groups. *Geotechnique*, 25(2), 159–174.

Poulos, H. G., & Davis, E. H. (1980). *Pile Foundation Analysis and Design*. Rainbom-Bridge Book Co.

Poulos, H. G., Small, J. C., & Chow, H. (2011). Piled raft foundations for tall buildings. *Geotechnical Engineering Journal of the SEAGS & AGSSEA*, 42(2), 78–84.

Rao, K., & Supriya, J. (2015). Design and construction of driven timber piles and foundations. *International Journal of Computer Engineering In Research Trends, 2(2),* 1020–1025.

Sherif, S. Abdel Salam, S., Suleiman, M. T., & Sritharan, S. (2012). Enhanced load-transfer analysis for friction piles using a modified borehole shear test. *Geotechnical Testing Journal*, 35(6), 879–889. Doi: 10.1520/GTJ20120071.

Sliwinski, Z. J., & Fleming, W. G. K. (1984). PAPER 15-The integrity and performance of bored piles. *In Piling and ground treatment* (pp. 211–223). Thomas Telford Publishing.

Vijayvergiya V. N. (1977). Load movement characteristics of piles. *Proceedings of Ports '77: the 4th annual symposium of the Waterway, Port, Coastal and Ocean Division of ASCE, ASCE,* New York, NY, USA, 269–284.

Yu, Y. W. (2009). *Pile driving analysis via dynamic loading test*. University of Southern Queensland.

Ouyang, Z., & Mayne, P. W. (2018). Effective friction angle of clays and silts from piezocone penetration tests. *Canadian Geotechnical Journal*, *55*(9), 1230–1247.